Carbon Vol. 28, No. 6, pp. 887–896, 1990
Printed in Great Britain.

0008-6223/90 $3.00 + .00

929

MODELS FOR ROUGHENING OF GRAPHITE DURING ITS CATALYZED GASIFICATION

JOSEPH M. RANISH† and PHILIP L. WALKER, JR.
Department of Materials Science and Engineering, The Pennsylvania State University, University Park, PA, 16802, U.S.A.

(*Received* 12 *September* 1989; *accepted in revised form* 16 *May* 1990)

Abstract—Models were developed to calculate porosities and total areas, and catalyzed to uncatalyzed gasification rate ratios as a function of burn-off for graphite flakes initially contaminated with channelling or pitting catalysts. The models indicate that small loadings of catalysts can increase the overall gasification rate by surface roughening without having a measurable effect due to interfacial catalysis.

Key Words—Models, roughening, catalyzed gasification, graphite.

1. INTRODUCTION

During a study of the kinetics of O_2 gasification of high purity graphite[1], interest was raised regarding the effects of trace levels of catalysts upon the active area and its development with burn-off. Although the effects of catalysts uncovered during gasification on the overall gasification rate have been studied[2], there have been no similar reports on the effects of trace levels of catalysts initially deposited on the surface upon the carbon morphology. This case would arise from contamination of a sample of airborne dust particles. It could also arise from attempts to change the porosity and surface area of a carbon by deliberate catalytic roughening. Studies of the behavior of catalyst particles during carbon oxidation are almost entirely based on the examination of the outer, mostly basal, surfaces of graphite crystals[3–10]. Catalyst particles do tunnel inside graphite[7,11]; but, perhaps due to the difficulty of performing these studies, the morphology change caused by these particles has not been characterized for oxidants. In the absence of this information, tunnelling morphology was assumed to be similar to channelling morphology. The studies performed on graphite basal surfaces reveal such complex morphology changes that realistic modelling only appears feasible using probabilistic approach. The current effort was focused instead upon much simpler analytic models that could be used to estimate the maximum effects caused by catalyst induced surface roughening. The models developed here are thus necessarily highly idealized and consider only the two modes of behavior producing the greatest roughness per amount of carbon gasified; namely, channelling (including tunnelling)* and pitting. These models were used to estimate the maximum increases in porosity, total surface, and active surface, as well as how these quantities might evolve during burn-off as a function of the catalyst loading, activity, and dispersion. Although the models were developed for graphite flakes, they can be extended to other bulk carbons by changing the carbon properties and by increasing the flake dimensions.

2. THEORY

2.1 *Background*

Catalysts can increase the overall gasification rate by at least three different mechanisms: interfacial, spillover, and roughness. The interfacial mechanism is a local action at the carbon-catalyst interface with the rate being related to the interfacial area. The exact details at the interface are not know, but in some systems involve a dissolution of the carbon by the catalyst. For high loadings of very active catalysts, this mechanism may dominate the overall rate. Spillover refers to the catalyst being active in dissociating O_2 and donating O species to the carbon. The O species migrate to labile carbon sites and react. Spillover is similar to a reactant pressure increase in that the surface O loading is increased. This mechanism is important for several metals because these metals enhance the gasification rate in O_2 but retard it in O[3]. The last mechanism for catalytic action, roughness, is more subtle and would not be considered catalytic if the gasification rate were normalized to the active area. Since this normalization is rare, it is important to be able to estimate the increase in active area due to roughening and how the amount of roughening will change with continued burning.

Only the interfacial mechanism can account for a significant development in roughness since its effects are localized to the catalyst particle. In the following, changes in the exterior carbon surface caused by catalytic gasification are used to infer changes in the

†Present Address: GE Lighting, Cleveland, Ohio, 44112, U.S.A.

*From here on, channelling will be used to refer to attack parallel to the basal plane of graphite and will include both tunnelling and channelling proper.

carbon interior. Two general types of behavior were reported earlier[4–6]: channelling and pitting. Channelling catalysts travel within the basal plane of graphite, accelerate gasification of edge atoms, and generally produce a channel in the basal plane. Sometimes a channelling particle will travel along an edge leaving it serrated[7]. Elements that exhibit channelling behavior during oxidation are: Co[3,4], Ni[4,7], Zn[8], and Pt[4,7]. Pitting catalysts travel normal to the basal plane, accelerate gasification of basal plane atoms, and produce a pit in the basal plane. Elements that exhibit pitting behavior during oxidation are: Fe[3,4], Ag[3,4], Mn[4], and Ti[3]. Furthermore, Pt, Au, Fe, and Ni particles, which produce channelling, will also produce pitting when positioned at a basal plane defect[7]. In this case the number of pits formed is very much dependent upon the concentration of defects in the basal plane, as well as the number and mobility of catalyst particles. Many other elements, including Pb, Mo, Ir, Rh, Ru, Pd, Ni, and Mn, have exhibited both channelling and pitting behavior during oxidation[3,4]. For either mode of behavior, the particle must be in contact with carbon edge atoms, either at the edge of the basal plane or at a defect within the basal plane[5,7,8]. Thus not every particle is a catalyst. Only Ag has been reported to catalyze gasification by pitting at perfect sites within the basal plane[10]. The elements given in the preceding examples do not reflect the active form of the catalyst, which can be the carbide, the oxide, or the metal itself. In addition to these types of behavior, the catalyst particle can wet the edge carbon atoms and catalyze edge recession over a broader region. Cu particles act in this fashion, simultaneously channelling, spreading along the channel sides, and becoming smaller[9]. Catalysts that wet the carbon are those that can form oxides of the required stability under the prevailing reaction conditions[12].

The width of the channel at the growing tip is equal to the catalyst particle diameter. Typically, the channel diameter increases with distance from the catalyst particle[4,7]. For non-wetting catalysts, the channel sides are widened by uncatalyzed gasification. These catalysts can be characterized by β, the channel length divided by the exterior channel half-width, which is a ratio of the catalyzed recession rate to the uncatalyzed recession rate. Measurements of β indicate that it depends upon not only the particular catalyst and temperature but also the catalyst particle size and channel depth[5,7]. For one catalyst, β ranged from 15 to 80 depending upon channel depth and particle size[7]. In reality, there exists a distribution of βs even for one type of catalyst at one temperature. In this paper, pitting catalysts will be characterized by γ, the pit depth divided by the pit radius. If the concentration of basal plane defects is high enough so as not to limit penetration of the next basal plane and the catalyst does not wet the surface, γ represents the ratio of the catalyzed recession rate to the uncatalyzed recession rate. Experiments indicate, however, that pitting (and γ) is a very strong function of the basal plane defect concentration with a typical value of γ being about five[7]. For either of the two basic morphologies, channelling or pitting, the maximum roughness per amount of carbon gasified is developed for the case where the particle remains intact and does not spread along the edge carbon atoms.

For either type of catalyst, the collection of channels or pits is approximated by an "average" channel or pit. Each model starts with the definition of the "average" pore morphology. From this definition, a relationship between pore size and uncatalyzed recession length is obtained. This permits the definition of burn-off, porosity, total active area (TASA), and total area as functions of the exterior pore size. In some cases, the exterior pore perimeters converge and a steady state value is achieved with respect to surface roughness. The average exterior pore size then assumes its maximum value. No further increases per flake are possible for pore volume, TASA, or total area beyond those calculated for the steady state value. Porosity will continue to increase due to the decrease in total flake volume from edge recession. In other cases, the catalyst particles reach the flake center or a flake boundary before the pore perimeters converge. Obviously, as the catalyst particles approach the flake center, pore coalescence and catalyst sintering become important. The increase in areas and pore volume with additional burn-off must diminish. The maximum development of these properties is not calculable with the present simple model. Calculations are stopped at the point of catalyst particle convergence. The values at this point represent approximate lower limits to the maximum attainable values.

2.2 *Assumptions*

As stated above, both models are developed for the case of maximum roughness per unit of carbon burn-off. To this end, both models assume that there are no mass transfer limitations, that all of the particles are active catalysts, and that the catalyst particles are unchanged during burn-off; no devolatilization, sintering, wetting and spreading, or deactivation are considered. Catalyst particles are assumed to burrow into the graphite normal to its surface. This restriction is more severe for channelling catalysts, which often travel in definite crystallographic directions[5,7]. It could be removed by the use of an equivalent β. Although both models ignore the effects of O_2 spillover, this effect is empirically accounted for in the measurements of β and γ when the surface oxide migration rate is high. These assumptions may be realized only in specific instances. The models are expected to be more accurate in predicting maximum effects and trends than in producing absolute numerical values. Because every catalyst particle is assumed to be producing maximum roughness, the model predictions

will underestimate the amount of burn-off required to achieve any given increase in surface area.

For convenience, both models employ the notion of an "average" pore, which represents the distribution of pores. The use of an "average" pore will cause the predicted evolution of areas and porosity with burn-off to be more abrupt than if a distribution of pores were used. Both models employ an idealized cylindrical disc of carbon, no reaction anisotropy within the basal plane, no uncatalyzed reaction normal to the basal plane, and no pore coalescence. The latter assumption is appropriate for low catalyst loadings. Both models assume that the catalyst particle size is negligible compared to the pore volume. This assumption becomes valid only after a very small amount of burn-off. The two models differ by mode of catalyst attack and the consequent pore geometry.

2.3 *Channelling catalysts*

Channelling catalysts are assumed to be uniformly distributed over the circumferential (edge) area of the graphite flake. As shown in Fig. 1, the flake has initial diameter, d_0, initial radius, r_0, and initial thickness, t_0. N particles of diameter, d_{cat}, radius, r_{cat}, tunnel into the flake parallel to the basal plane at β times the uncatalyzed recession rate of the flake edges. To prevent catalyst sintering, the particles must be separated from each other (i.e., the total area of the particles projected onto the edge surface must be a small fraction of the edge surface). The pore produced is depicted in Fig. 2 where an untypically low β was used for clarity. The pore volume equals that of the two triangular areas created by uncatalyzed recession plus the rectangular volume swept out by the catalyst particle minus half the volume of the catalyst particle. The volume of half the catalyst particle will be ignored in this treatment. This approximation becomes more accurate as the volume of the catalyst particle becomes a smaller fraction of the pore volume, which will be increasingly satisifed as gasification proceeds.

From Fig. 2, the pore half-width, r_p, is related to the uncatalyzed recession length, u, by

$$r_p = (\beta - 1)\, u/\beta + r_{cat}. \quad (1)$$

At this time the flake radius, r, is reduced from the initial value, r_0 by the uncatalyzed recession, u. Using eqn 1 to substitute for u, yields

$$r = r_0 - \beta(r_p - r_{cat})/(\beta - 1). \quad (2)$$

At each channel, new edge area is created along the two sides of the wedge from carbon exposed as the catalyst particle passes. At the same time, initial edge area at the flake circumference is lost as the mouth of the channel opens due to uncatalyzed gasification. The net increase in total active surface area, TASA, per channel is given by

$$\text{TASA/channel} = 2\sqrt{1 + \beta^2}(r_p - r_{cat})2r_{cat} - 4r_{cat}r_p = 4r_{cat}[\sqrt{1 + \beta^2}(r_p - r_{cat}) - r_p]. \quad (3)$$

The TASA per flake is the sum of the edge TASA, $2\pi t_0 r$, plus N times the TASA increase per channel given by eqn 3. Using eqn 2 to express r, this yields

$$\text{TASA/flake} = 2\pi t_0 \left[r_0 - \frac{\beta}{\beta - 1}(r_p - r_{cat}) \right] + 4Nr_{cat}\left[\sqrt{1 + \beta^2}(r_p - r_{cat}) - r_p \right]. \quad (4)$$

In each channel, new basal area is created, none is lost. The increase in basal area per channel is

$$\text{basal area/channel} = 2(r_p - r_{cat})^2\beta + 2\beta(r_p - r_{cat})d_{cat} = 2\beta(r_p^2 - r_{cat}^2). \quad (5)$$

The total basal area per flake is then the sum of the exterior basal area, $2\pi r^2$, plus that created within the channels as given by eqn 5. Using eqn 2 to express r, this yields

$$\text{basal area/flake} = 2\pi \left[r_0 - \frac{\beta}{\beta - 1}(r_p - r_{cat}) \right]^2 + 2N\beta\,(r_p^2 - r_{cat}^2). \quad (6)$$

The volume within each channel is half the total basal area of the channel, which is given by eqn 5, times

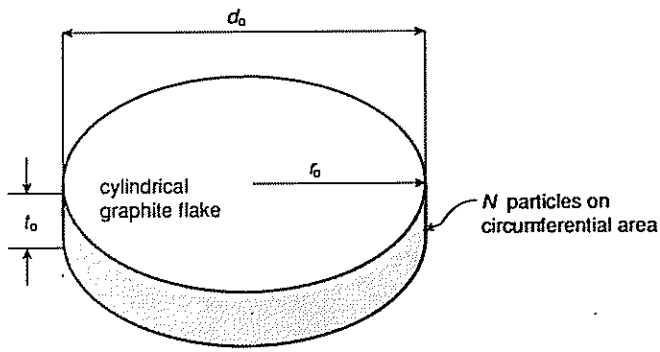

Fig. 1. Channelling catalyst geometry. (Not to scale.)

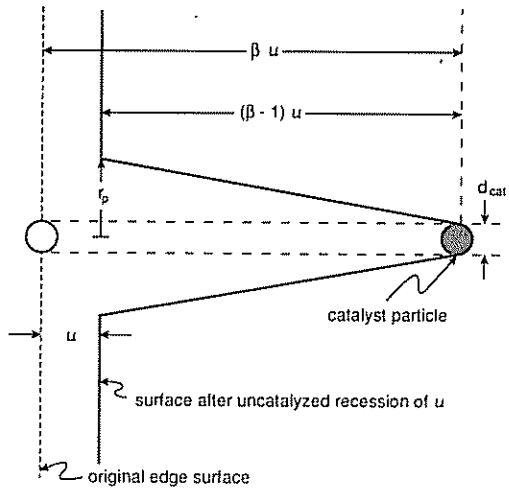

Fig. 2. Channelling catalyst pore geometry. (View normal to basal plane. Not to scale.)

the channel height, $2r_{cat}$, or

$$\text{volume in channel} = 2r_{cat}\,\beta(r_p^2 - r_{cat}^2). \quad (7)$$

Without channels, the flake volume would be $\pi r^2 t_0$ or using eqn 2 to substitute for r

$$\text{total flake volume} = \pi\,[r_0 - \beta(r_p - r_{cat})/(\beta - 1)]^2 t_0. \quad (8)$$

The flake porosity is the volume in the N channels divided by the total flake volume or

$$\text{porosity} = \frac{N2r_{cat}\beta(r_p^2 - r_{cat}^2)}{\pi[r_0 - \beta\,(r_p - r_{cat})/(\beta - 1)]^2 t_0}. \quad (9)$$

The burn-off for a flake initially 100% dense is the volume lost divided by the initial volume or

$$\text{burn-off} = \frac{\pi t_0\{r_0^2 - [r_0 - \beta(r_p - r_{cat})/(\beta - 1)]^2\} + N2r_{cat}\beta(r_p^2 - r_{cat}^2)}{\pi r_0^2 t_0}. \quad (10)$$

The factor containing the "{ }" brackets in the numerator of eqn 10 represents the volume of carbon lost by recession of the flake periphery; the other factor represents the volume of carbon lost in creating the channels.

As the pore mouths on the flake circumference converge, the increase in roughness with additional burn-off will diminish. No further increase in roughness with burn-off will occur when the pore mouths completely cover the circumferential area of the flake. Because the pore mouths are oriented on the edge of the graphite flake and only grow circumferentially (in the direction normal to the catalyst recession direction), the steady state roughness criterion depends on the arrangement of the catalyst particles on the surface. Referring to Fig. 3, if m is the number of catalyst particles within a band d_{cat} at the same height around the flake circumference, the pore mouths will approximately cover the circumferential area when the edges of the m pore mouths equal the flake circumference or

$$m2r_p = 2\pi r, \quad \text{where } m \le N. \quad (11)$$

If $m = N$, the total number of catalyst particles on a flake, then the burn-off to steady state roughness will be a minimum. As m decreases, more burn-off will be required to reach steady state. For randomly distributed particles, a good statistical approach is

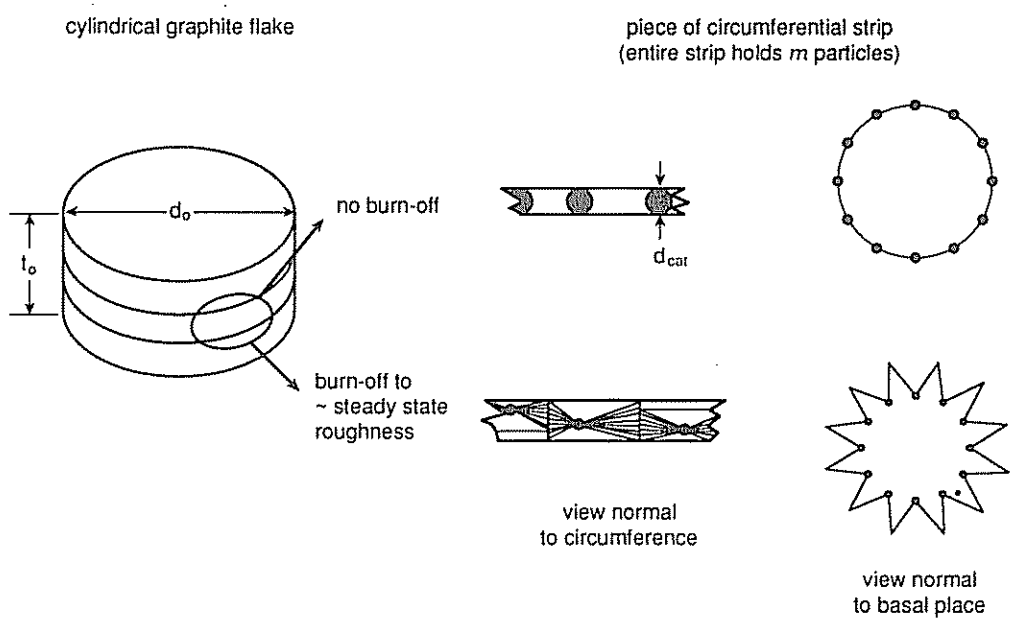

Fig. 3. Steady state roughness for channelling catalyst. (Not to scale.)

required to determine the criterion for steady state roughness. An approximate solution, however, is to use eqn 11 with m equal to the average number of particles in a circumferential strip d_{cat} wide, or

$$m = \left(\frac{N}{2\pi r_0 t_0}\right)(d_{cat} 2\pi r_0) = \frac{2Nr_{cat}}{t_0} \quad . \qquad (12)$$

With this value of m, eqn 11 indicates that steady state roughness will be reached approximately when

$$4Nr_{cat} r_p / t_0 = 2\pi r. \qquad (13)$$

The same expression results when the total area of the channel mouths equals the current circumferential (edge) area. Combining eqn 13 with eqn 2 yields the expression for r_p at steady state,

$$r_{p,ss} = \frac{r_0 + \dfrac{\beta}{\beta - 1} r_{cat}}{\dfrac{2Nr_{cat}}{\pi t_0} + \dfrac{\beta}{\beta - 1}} \quad . \qquad (14)$$

Because $r_0 \gg \dfrac{\beta}{\beta - 1} r_{cat}$, eqn 14 can be reduced to

$$r_{p,ss} = \frac{r_0}{\dfrac{2Nr_{cat}}{\pi t_0} + \dfrac{\beta}{\beta - 1}} \quad . \qquad (15)$$

In order for steady state roughness to be achieved before the flake burns out, $u < r_0$. A more restrictive condition is that the depth to which the particles recede must not extend beyond the radius at which all particles would be touching. Alternatively, one could ignore sintering if the distance from the flake center to the particle is at least k_p times the radius at which the particles would be touching or

$$r_0 - \beta u \geq k_p \frac{m d_{cat}}{2\pi} = k_p \frac{2Nr_{cat}^2}{\pi t_0} \quad . \qquad (16)$$

The value of k_p is chosen to limit the error caused by catalyst sintering. Using eqn 1 to replace u in Inequality 16 yields the constraint on the exterior channel half-width

$$r_p \leq \left(\frac{\beta - 1}{\beta^2}\right)\left(r_0 - \frac{2k_p Nr_{cat}^2}{\pi t_0}\right) + r_{cat}. \qquad (17)$$

As r_p approaches the right-hand side of Inequality 17, the effects of catalyst particle sintering and pore coalescence become more severe and the model predictions become more inaccurate.

In the preceding treatment, half the catalyst particle occupied some of the channel volume. In order to neglect the catalyst particle size, it must be small compared to the channel volume. If negligible error is introduced when the channel volume is k_s times larger than half the particle volume, the condition of negligible catalyst volume now can be stated more explicitly. The channel volume, given by eqn 7, must then be at least k_s times larger than half the catalyst particle volume, which is $2\pi r_{cat}^3/3$,

$$2r_{cat}\beta(r_p^2 - r_{cat}^2) \geq k_s 2\pi r_{cat}^3/3. \qquad (18)$$

Rearranging Inequality 18, the catalyst particle is considered negligible when enough burn-off has occurred so that

$$r_p \geq \sqrt{\frac{k_s \pi/3 + \beta}{\beta}}\, r_{cat}. \qquad (19)$$

For large values of β, Inequality 19 is satisfied at very low amounts of uncatalyzed recession.

When Inequality 17 is satisfied, then $r_p - r_{cat} < r_0$ and, for $\beta > 1$, eqns 4, 6, 9, 10, and 15 can be simplified by neglecting $\beta(r_p - r_{cat})/(\beta - 1)$ with respect to r_0. The resulting equations are given below as eqns 20 to 24.

$$\text{TASA/flake} = 2\pi t_0 r_0 + 4Nr_{cat}[\beta(r_p - r_{cat}) - r_p] \qquad (20)$$

$$\text{basal area/flake} = 2\pi r_0^2 + 2N\beta(r_p^2 - r_{cat}^2) \qquad (21)$$

$$\text{porosity} = \frac{2N\beta r_{cat}(r_p^2 - r_{cat}^2)}{\pi r_0^2 t_0} \qquad (22)$$

$$\text{burn-off} = \frac{2N\beta r_{cat}(r_p^2 - r_{cat}^2)}{\pi r_0^2 t_0} = \text{porosity} \qquad (23)$$

$$r_{p,ss} = \frac{\pi t_0 r_0}{2Nr_{cat}} \quad . \qquad (24)$$

The maximum relative increases in TASA, basal area, and pore volume (expressed as porosity), and the burn-off required to reach steady state can now be calculated for the valid region of the model for large β. Combining eqns 20 and 24 and normalizing to the initial TASA, TASA_0, yields

$$\text{TASA/TASA}_0 = \beta\left(1 - \frac{2Nr_{cat}^2}{\pi r_0 t_0}\right) \quad . \qquad (25)$$

Equation 25 shows that the maximum relative increase in TASA is β and this maximum is achieved when the catalyst size is negligible or the number of catalyst particles is small. Similarly, the maximum increase in basal area relative to the initial basal area may be obtained from eqns 21 and 24 as,

$$\text{basal/basal}_0 = 1 + \frac{\pi t_0^2 \beta}{4Nr_{cat}^2} - \frac{N\beta r_{cat}^2}{\pi r_0^2} \qquad (26)$$

Substituting eqn 24 into eqn 23 yields corresponding steady state values for the porosity and burn-off given by eqn 27.

$$\text{porosity}_{ss} = \text{burn-off}_{ss} = \frac{\pi t_0 \beta}{2Nr_{cat}} - \frac{2N\beta r_{cat}^3}{\pi r_0^2 t_0} \quad . \qquad (27)$$

2.4 *Pitting catalysts*

Model development for pitting catalysts follows the same approach as for channelling catalysts, except that the pore geometry is different. Here, N catalyst particles are uniformly distributed on the basal area of the graphite flake ($N/2$ on each basal face) and tunnel normally inward at a rate γ times the edge recession rate. This leads to a pore shaped like the frustum of a cone as shown in Fig. 4. According to this view, the pit sides are composed of steps of alternating edge area and basal area. The fraction of the lateral area that is edge area is equal to $\gamma/\sqrt{1+\gamma^2}$.

Because the catalyst free portion of the original basal surface does not recede, Fig. 4 indicates that

$$r_p = u + r_{cat}. \tag{28}$$

The TASA increase per pit, given by eqn 29, is the pit lateral area times the fraction of it that is edge area.

$$\text{TASA/pit} = \pi(r_p + r_{cat}) \times \sqrt{\gamma^2 r_p^2 + (r_p - r_{cat})^2}\,\frac{\gamma}{\sqrt{1+\gamma^2}}. \tag{29}$$

This leads to a TASA per flake of

$$\text{TASA flake} = 2\pi t_0(r_0 - r_p + r_{cat}) + N\pi(r_p + r_{cat}) \times \sqrt{\gamma^2 r_p^2 + (r_p - r_{cat})^2}\,\frac{\gamma}{\sqrt{1+\gamma^2}}. \tag{30}$$

Pitting causes no change in the basal area. The basal area created inside the pit equals the basal area lost at the exterior mouth of the pit. The basal area per flake is reduced only by the recession of the flake circumference and is given by

$$\text{basal area/flake} = 2\pi(r_0 - r_p + r_{cat})^2. \tag{31}$$

The porosity per flake is N times the pit volume divided by the current flake volume or

$$\text{porosity} = \frac{N\gamma r_p(r_p^2 + r_p r_{cat} + r_{cat}^2)}{3t_0(r_0 - r_p + r_{cat})^2}. \tag{32}$$

This porosity plus the volume loss associated with the edge recession yield a burn-off given by

$$\text{burn-off} = \frac{t_0[r_0^2 - (r_0 - r_p + r_{cat})^2] + N\gamma r_p(r_p^2 + r_p r_{cat} + r_{cat}^2)/3}{r_0^2 t_0}. \tag{33}$$

A steady state roughness will result when the exterior pore radii converge, which will happen approximately when the area of the N pore mouths equals the basal area, or

$$N\pi r_{p,ss}^2 = 2\pi(r_0 - r_{p,ss} + r_{cat})^2. \tag{34}$$

For this r_p to be a reasonable value, the catalyst particle must be within the flake or, in terms of r_p,

$$r_p < t_0/\gamma. \tag{35}$$

Additionally, in order to avoid the complication caused by catalysts being undercut by the receding flake circumference, the uncatalyzed recession depth should be set so that the reduction in basal plane area is less than 10%, or

$$r_p < (1 - \sqrt{0.9})r_0. \tag{36}$$

The more restrictive of these two constraints is usually keeping the catalysts within the flake, because t_0/γ is less than $(1 - \sqrt{0.9})r_0$. Once a steady state roughness condition is established, the assumption that the basal plane does not recede is no longer valid; and the model equations must be modified.

The pitting model is valid only when Inequalities 35 and 36 are obeyed, and under these conditions $r_p \ll r_0$. Because $r_{cat} \leq r_p$, $r_{cat} \ll r_0$. Therefore, simpler expressions for the areas, porosity, burn-off, and $r_{p,ss}$ can be obtained by ignoring r_p and r_{cat} relative to r_0 in eqns 30 to 34. After rearranging eqn 34, this results in eqns 37 to 41 below.

$$\text{TASA/flake} = 2\pi t_0 r_0 + N\pi(r_p + r_{cat}) \times \sqrt{\gamma^2 r_p^2 + (r_p - r_{cat})^2}\,\frac{\gamma}{\sqrt{1+\gamma^2}} \tag{37}$$

$$\text{basal area/flake} = 2\pi r_0^2 \tag{38}$$

$$\text{porosity} = \frac{N\gamma r_p(r_p^2 + r_p r_{cat} + r_{cat}^2)}{3t_0 r_0^2} \tag{39}$$

$$\text{burn-off} = \frac{N\gamma r_p(r_p^2 + r_p r_{cat} + r_{cat}^2)}{3t_0 r_0^2} \tag{40}$$

$$r_{p,ss} = r_0\sqrt{2/N}. \tag{41}$$

Under conditions valid for this model, negligible burn-off occurs by recession of the flake edges; es-

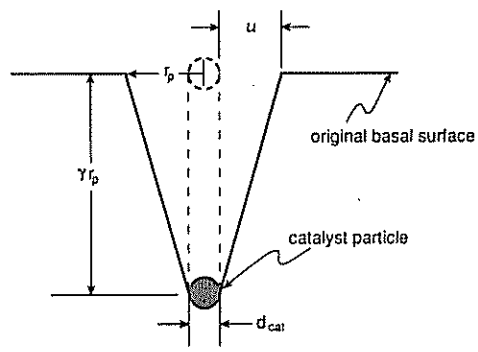

Fig. 4. Pitting catalyst pore geometry. Cross section through basal plane. View normal to circumference. (Not to scale.)

sentially all the burn-off occurs within the pores. Hence, the burn-off and porosity are identical.

The maximum TASA developed relative to the initial TASA, $TASA_0$, is calculated by substituting $r_{p,ss}$ from eqn 41 into eqn 37 and normalizing by $TASA_0$.

$$\mathrm{TASA/TASA_0} = 1 + N\frac{r_0\sqrt{2/N} + r_{cat}}{2r_0t_0} \times \sqrt{\gamma^2 2r_0^2/N + \left(r_0\sqrt{2/N} - r_{cat}\right)^2}\frac{\gamma}{\sqrt{1+\gamma^2}}. \quad (42)$$

The basal area at steady state roughness is identical to the initial basal area. The porosity and burn-off at steady state, obtained by substituting eqn 41 in eqn 39 or eqn 40 are found to be equal and given by

$$\mathrm{porosity_{ss}} = \mathrm{burn\text{-}off_{ss}} = \frac{N\gamma r_0\sqrt{2/N}(2r_0^2/N + r_0r_{cat}\sqrt{2/N} + r_{cat}^2)}{3t_0r_0^2}. \quad (43)$$

3. DISCUSSION

Table 1 summarizes and compares the steady state roughness values of TASA, basal area, porosity, burn-off, and uncatalyzed recession for both catalyst types under the conditions, $\beta \gg 1$, $\gamma \gg 1$, and $r_p \gg r_{cat}$. Table 1 can be used to estimate the maximum effects of catalytic roughening. For channelling catalysts, the quantity $\pi t_0/(2r_{cat}N)$ appears frequently; so many of the quantities could be expressed equally well in terms of steady state porosity. For pitting catalysts, $r_0\gamma/t_0$ appears frequently; so many quantities could be expressed in terms of $TASA/TASA_0$. Uncatalyzed recession, which is linearly related to time, is included in order to make time and global rate comparisons.

Table 1. Values at steady state roughness

Parameter	Channelling	Pitting
$TASA/TASA_0$	β	$r_0\gamma/t_0$
$basal/basal_0$	$1 + \pi t_0^2\beta/(4r_{cat}^2N)$	1.0
porosity	$\pi t_0\beta/(2r_{cat}N)$	$2\sqrt{2}r_0\gamma/(3\sqrt{N}t_0)$
burn-off	$\pi t_0\beta/(2r_{cat}N)$	$2\sqrt{2}r_0\gamma/(3\sqrt{N}t_0)$
u	$\pi t_0 r_0/(2r_{cat}N)$	$\sqrt{2/N}r_0$

The major differences between the catalyst types arise from pit morphology and flake morphology. All the area created in the pit is TASA, whereas only part of the area created in the channel is TASA. For the same catalyst activity, the ratio of TASA created by pitting catalyst particles to TASA created by channelling catalyst particles is r_0/t_0. For graphite flakes where $r_0 > t_0$, pitting catalysts are more effective in increasing TASA than channelling catalysts. If increases in basal area are desired, however, the only choice is to use a channelling catalyst. For either catalyst type, the relative increase in TASA at steady state roughness does not depend upon the catalyst loading for active catalysts. For active catalysts, the TASA development is dominated by TASA developed within the pores. For either pore geometry, the ratio of TASA inside the pore to the area of the pore mouth is a constant. At steady state roughness, the area of all the pore mouths approximately equals the area bounding either the basal planes for pitting catalyst particles or the circumferential area for channelling catalyst particles. The TASA at steady state thus becomes a constant times the appropriate bounding area, which is independent of the number of pores or catalyst loading. However, the catalyst loading or N is important in determining the amount of burn-off required to reach steady state roughness, because less burn-off is required for pore mouth convergence when there are more pores. It is possible to have a catalyst loading that is insufficient to affect the global rate via interfacial attack, yet have a dramatic effect on the global rate via roughening. Furthermore, because the TASA and basal area have different functional dependencies, the fraction of the total area that is TASA, in general, does not remain constant during the burn-off to steady state roughness. The ratio of total area to TASA is 1 + (basal area)/TASA. This ratio is initially $1 + r_0/t_0$ for a smooth (unpitted) graphite flake but changes to $1 + 1/\gamma$ for a flake at a steady state roughness induced by basal plane pitting or $1 + r_0/t_0[1/\beta + \pi t_0^2/(4r_{cat}^2N)]$ for a flake at a steady state roughness induced by edge channelling. In either case, the initial ratio of areas is not preserved. These results dramatize the need for making TASA measurements frequently during burn-off if reactivities are to be normalized to TASA.

3.1 *Application to SP-1 graphite*

For illustrative purposes the models were applied to a representative flake of SP-1 graphite having the characteristics exhibited in Table 2. In order to facilitate relative comparisons between the two types of catalysts, the catalyst particle surface concentration and the catalyzed to uncatalyzed recession rate ratio for the edge plane will be set equal to those of

Table 2. Characteristics of SP-1 graphite typical flake

flake diameter	2.92×10^{-5} m
flake thickness	5.00×10^{-7} m
density	2.265×10^{3} Kg/m^3
initial volume	3.348×10^{-16} m^3
initial weight	7.584×10^{-13} Kg
initial TASA	4.587×10^{-11} m^2, 3.31 % of total area
initial total area	1.385×10^{-9} m^2, 1.826 m^2/g

the basal plane. The graphite flake is assumed to be uniformly contaminated with 20 ppm of a catalyst having a density of 2.0×10^3 Kg/m^3, diameter of 2.0 nm, and β and γ of 20. The basal area will be contaminated with 96.69% of the total number of catalyst particles, the edge area will be contaminated with the remaining 3.31%.

Catalyst properties are interrelated by eqns 44 to 46. CATTASA is the projected total catalyst area onto the carbon of one flake. Equation 46 shows how the ratio of the catalyzed gasification rate to the uncatalyzed gasification rate is calculated.

$$N = 1.5\left(\frac{\text{graphite density}}{\text{catalyst density}}\right)\left(\frac{\text{weight of catalyst}}{\text{weight of graphite}}\right)\left(\frac{r_0^2 t_0}{2r_{cat}^3}\right) \quad (44)$$

$$\text{CATTASA} = N\pi r_{cat}^2 \quad (45)$$

$$R_c/R_u = \text{CATTASA } \beta \text{ (or } \gamma)/\text{TASA} \quad (46)$$

Applying these equations along with the exact equations to the case at hand yields values given in Table 3. As expected, these values agree well with those in Table 1. The steady state values for burn-off are slightly higher than the corresponding values for porosity due to the contribution from edge recession. *Table 3 clearly shows that for ppm levels of catalysts initially deposited on SP-1, the global reaction rate increases mainly by virtue of a TASA increase and not by virtue of the direct interfacial catalyst attack.* (Additionally, the TASA may recede faster than the TASA in an uncatalyzed case due to O_2 spillover.) Considering only the edge area to be contaminated, Table 3 indicates that the interfacial gasification rate is initially 8.18% of the uncatalyzed rate and decreases by a factor of 20 to about 0.42% entirely as a result of the increase in TASA. Although the interfacial rate becomes less significant with burn-off, the global rate increases with burn-off by the same factor of 20 as a result of catalytically induced roughening. Considering only the basal area to be contaminated at the same catalyst surface density as the edge area, the results in Table 3 are even more dramatic. The initial interfacial gasification rate is 2.4 times the uncatalyzed rate, but decreases by a factor of ~620 to about 0.4% of the uncatalyzed rate, again entirely because of the increase in TASA. The global rate increases by a factor of ~620 during the burn-off to steady state roughness. The pitting catalyst interfacial rate becomes completely dominated by the catalytically induced roughening of the TASA. The total area increase for the pitting catalyst is less than that for the channelling catalyst, because only TASA is created by the pitting catalyst. In both of these cases, essentially all the burn-off occurs within the catalyst created pores. Using the uncatalyzed recessions to reflect time, the pitting catalyst achieves 44% burn-off in about one tenth the time in which the channelling catalyst achieves 28% burn-off.

The numerical results in Table 3 for SP-1 graphite show that the total area does not increase by the same proportion as the TASA. For the channelling catalyst, the total area increased about three times more than did the TASA. For the pitting catalyst, the TASA increased about thirty times more than did the total area.

The approach to steady state roughness is illustrated in Fig. 5 for the channelling catalyst and pitting catalyst cases as described in Table 3. In order to neglect the volume of the catalyst particle relative to the pore volume, burn-offs greater than 0.03% are required for the channelling catalyst, and burn-offs greater than 0.3% are required for the pitting catalyst. For burn-offs less than these, the calculated TASA and calculated total area will be too high. In either case, all the values will increasingly approach the calculated ones as the burn-off progresses. The uncatalyzed case is shown for comparison. As ex-

Table 3. SP-1 graphite contaminated with 20 ppm catalyst

	Edge	Basal
Number of Catalyst Particles	5.97×10^4	1.74×10^6
Particle Surface Density, m^{-2}	1.30×10^{15}	1.30×10^{15}
CATTASA/TASA$_0$	4.09×10^{-3}	1.20×10^{-1}
$(R_c/R_u)_{initial}$	8.18×10^{-2}	2.40
Conditions at Steady State Roughness		
Uncatalyzed Recession, m	1.88×10^{-7}	1.46×10^{-6}
Burn-off, %	28.3	45.1
Porosity, %	26.3	44.6
TASA/Initial TASA	19.6	622.3
Total Area/Initial Total Area	63.4	21.6
(R_c/R_u)	4.16×10^{-3}	3.85×10^{-3}

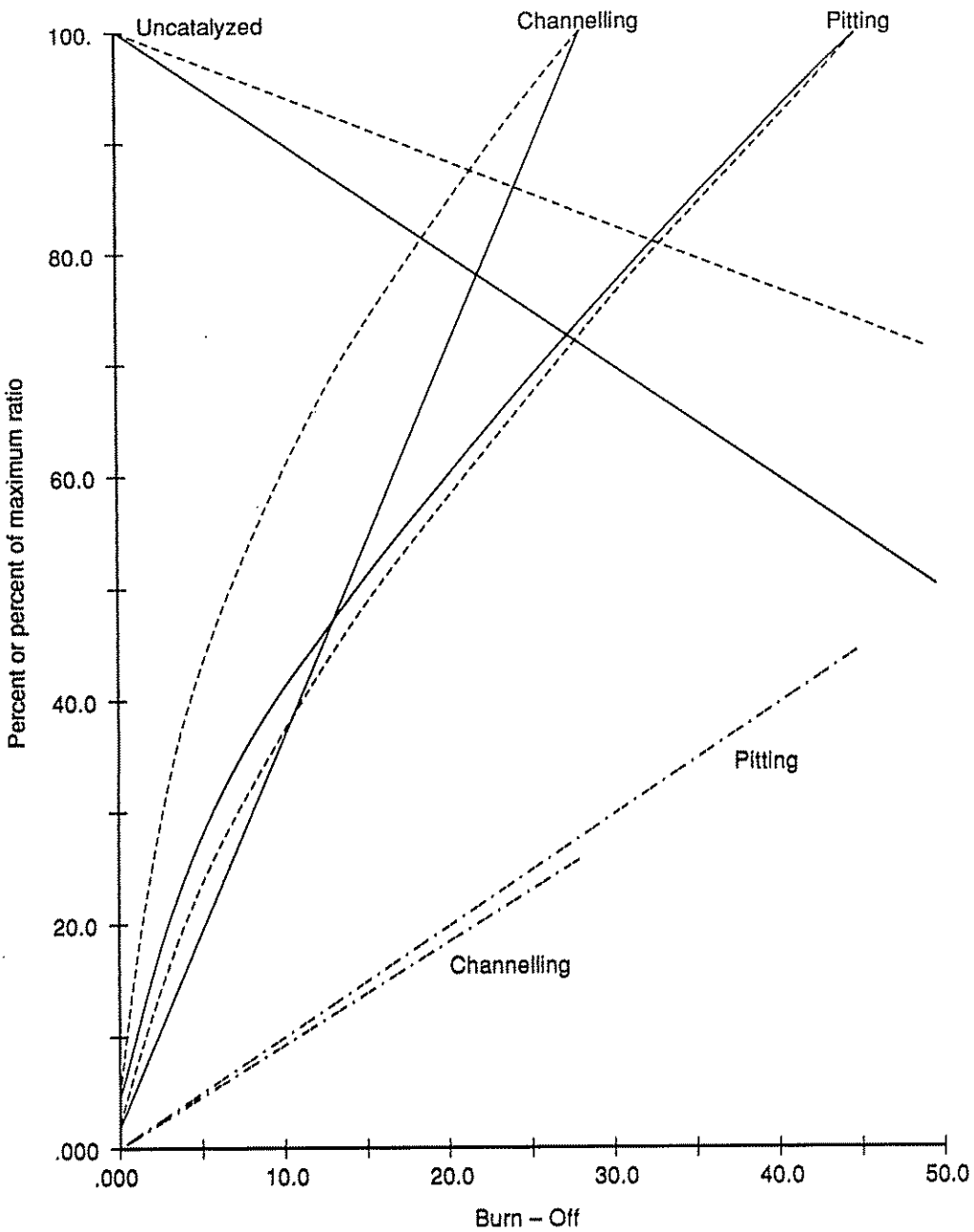

Fig. 5. Area and porosity development with burn-off: ———total area/initial total area as percent of Table 3 maximum; - - - - TASA/initial TASA as percent of Table 3 maximum; -- · -- porosity.

pected from the equations, the total area and TASA developed by catalytic roughening are roughly linear functions of the burn-off up to steady state roughening. This is in contrast to the roughly linear decrease in TASA and total area with burn-off for the uncatalyzed case. Over the range of burn-off in Fig. 5, the porosity and burn-off are almost identical.

4. SUMMARY

Simple models were developed to calculate the porosity, total area, total active area, and catalyzed to uncatalyzed gasification rate ratio as a function of burn-off for graphite contaminated with channelling or pitting catalysts. The models were applied to SP-1 graphite and showed that small loadings of catalysts could increase the overall gasification rate by surface roughening, which increases the uncatalyzed rate in proportion to the active surface increase, without having a measurable affect on the rate due to interfacial catalysis. These results dramatize the need for making TASA measurements frequently during burn-off if reactivities are to be accurately expressed in terms of TASA.

Acknowledgements—This research was supported by the Division of Chemical Sciences, Office of Basic Energy Sciences, U.S. Department of Energy on Contract No. DE-AC02-79ER 10488.

REFERENCES

1. J. M. Ranish Ph.D Thesis, The Pennsylvania State University (1984).
2. C. Heuchamps and X. Duval, *Carbon* **4**, 243 (1966).
3. J. M. Thomas, Microscopic studies of graphite oxidation. In *The Chemistry and Physics of Carbon* (Edited by P. L. Walker, Jr.), Vol. 1, p. 121. Marcel Dekker, New York (1965).
4. D. W. McKee, *Carbon* **8**, 623 (1970).
5. R. T. K. Baker, Controlled atmosphere electron microscopy of gas-solid interactions. In *Chemistry and Physics of Solid Surfaces* (Edited by R. Vanselow and S.Y. Tong) Vol. 1, p. 293. CRC Press, Cleveland (1977).
6. G. R. Hennig, *Proc. of the Fifth Conference on Carbon*, Vol. 1, p. 143, Pergamon Press, New York (1962).
7. G. R. Hennig, *J. Inorg. Nucl. Chem.* **24**, 1129 (1962).
8. R. T. K. Baker and P. S. Harris, *Carbon*, **11**, 25 (1973).
9. R. T. K. Baker and J. J. Chludzinski, Jr., *Carbon*, **19**, 75 (1981).
10. P. S. Harris, F. S. Feates, and B. G. Reuben, *Carbon*, **12**, 189 (1974).
11. P. J. Goethel and R. T. Yang, Extended Abstracts, 19th Biennial Conference on Carbon, p. 578, University Park, PA (1989).
12. R. T. K. Baker, *Carbon*, **24**, 715 (1986).